



Estimation of evapotranspiration by FAO Penman-Monteith Temperature and Hargreaves-Samani models under temporal and spatial criteria. A case study in Duero Basin (Spain).

5 Rubén Moratíel^{1,2}, Raquel Bravo³, Antonio Saa^{1,2}, Ana M Tarquis², Javier Almorox¹

¹Department of Plant Production, Universidad Politécnica de Madrid, Avda. Complutense s/n, Madrid 28040, Spain

²CEIGRAM, Centro de Estudios e Investigación para la Gestión de Riesgos Agrarios y Medioambientales, C/Senda del Rey 13, Madrid, 28040, Spain

³Ministerio de Agricultura y Pesca, Alimentación y Medio Ambiente Paseo de la Infanta Isabel 1, Madrid, 28071, Spain

Correspondence to: Rubén Moratíel (ruben.moratíel@upm.es)

15

Abstract. Use of the Evapotranspiration based scheduling method is the most common one for irrigation programming in agriculture. There is no doubt that the estimation of the reference evapotranspiration (ET_0) is a key factor in irrigated agriculture. However, the high cost and maintenance of agrometeorological stations and high number of sensors required to estimate it creates a non-plausible situation especially in rural areas. For this reason the estimation of ET_0 using air temperature, in places where wind speed, solar radiation and air humidity data are not readily available, is particularly attractive. Daily data record of 49 stations distributed over Duero basin (Spain), for the period 2000-2018, were used for estimation of ET_0 based on seven models against Penman-Monteith FAO 56 with temporal (annual or seasonal) and spatial perspective. Two Hargreaves-Samani models (HS), with and without calibration, and five Penman-Monteith temperature models (PMT) were used in this study. The results show that the models' performance changes considerably depending on whether the scale is annual or seasonal. The performance of the seven models was acceptable from an annual perspective ($R^2 > 0.91$, $NSE > 0.88$, $MAE < 0.52 \text{ mm} \cdot \text{d}^{-1}$ and $RMSE < 0.69 \text{ mm} \cdot \text{d}^{-1}$). For winter, no model showed a good performance. In the rest of the seasons, the models with the best performance were three: PMT_{CUH} , HS_C and PMT_{OUH} . HS_C model presents a calibration of Hargreaves empirical coefficient (k_{RS}). In PMT_{CUH} model, k_{RS} was calibrated and average monthly values were used for wind speed, maximum and minimum relative humidity. Finally, PMT_{OUH} model is as PMT_{CUH} model except that k_{RS} was not calibrated. These results are very useful to adopt appropriate measures for an efficient water management, especially in the intensive agriculture in semi-arid zones, under the limitation of agrometeorological data.

35



1. Introduction

40 Grow population and its demand for food increasingly demand natural resources such as water. This, linked with the uncertainty of climate change, makes water management a key point for future food security. The main challenge is to produce enough food for a growing population that is directly affected by the challenges set in the management of agricultural water, mainly with irrigation management (Pereira, 2017).

45 Evapotranspiration (ET) is the water lost from the soil surface and surface leaves by evaporation and, by transpiration, from vegetation. ET is one of the major components of the hydrologic cycle and represented as a loss of water from the drainage basin. Evapotranspiration (ET) information is key to understanding and managing water resources systems (Allen et al., 2011). ET is normally modeled using weather data and algorithms that describe aerodynamic characteristics of the vegetation and surface energy.

50 In agriculture, irrigation water is usually applied based on the water balance method in the soil water balance equation allows calculating the decrease in soil water content as the difference between outputs and inputs of water to the field. In arid areas where rainfall is negligible during the irrigation season an average irrigation calendar may be defined a priori using mean ET values (Villalobos et al., 2016). The Food and Agricultural Organization of United Nations (FAO) improved and upgraded the methodologies for reference evapotranspiration (ET_o) estimation by introducing the reference crop (grass) concept, described by FAO Penman- Monteith (PM- ET_o) equation (Allen et al., 1998). This approach was tested well under different climates and time step calculations and is currently adopted worldwide (Allen et al., 1998, Todorovic et al., 2013; Almorox et al., 2015). To estimate crop evapotranspiration (ET_c) is obtained by function of two factor ($ET_c = K_c \cdot ET_o$): reference crop evapotranspiration (ET_o) and crop coefficient (K_c) (Allen et al. 1998). ET_o was introduced to study the evaporative demand of the atmosphere independently of crop type, crop stage development and management practices. ET_o is affecting only for climatic parameters. Consequently, ET_o is considered a climatic parameter and is computed from weather data. The specific crop and climate characteristics influences in K_c values.

65 The ET is very variable locally and temporarily because of the climate. Because the ET component is relatively large in water hydrology balances any small error in its estimate or measurement represents large volumes of water (Allen et al., 2011). Small deviations in ET_o estimations would affect irrigation and water management in rural areas in which crop extension is significant. For example, in 2017 there was a water shortage at the beginning of the campaign (March) at the Duero basin (Spain). The classical irrigated crops, i.e. corn, were replaced by others with lower water needs such as sunflower.

70 Wind speed (U), solar radiation (Rs), relative humidity (RH) and temperature (T) of the air are required to estimate ET_o . Additionally, vapor pressure deficit (VPD), soil heat flux (G) and net radiation (Rn) measurements or estimates are necessary. The PM- ET_o methodology presents the disadvantage that required climate or weather data that are normally unavailable or low quality (Martinez and Thepadia, 2010) in rural areas. In this case, where data are missing, Allen et al. (1998) in the guidelines for PM- ET_o recommend two approaches: a) using equation of Hargreaves-Samani (Hargreaves and Samani, 1985) and 75 b) using PM temperature (PMT) method that requires data of temperature to estimate Rn (net radiation)



and VPD for obtaining ET_0 . In these situations, temperature-based evapotranspiration (TET) methods are very useful (Mendicino and Senatore, 2012). Air temperature is the most available meteorological data, which are readily from most of climatic weather station. Therefore, TET methods and temperature
80 databases are solid base for ET estimation all over the world including areas with limited data resources (Droogers and Allen, 2002).

Todorovic et al., (2013) reported that, in Mediterranean hyper-arid and arid climates PMT and HS show a similar behavior and performance while for moist sub-humid areas the best performance was obtained by PMT method. This behavior was reported for moist sub-humid areas in Serbia (Trajovic, 2005). Several
85 studies confirm this performance in a range of climates (Martinez and Thepadia, 2010; Raziei and Pereira, 2013; Almorox, et al. 2015; Ren et al. 2016). Both models (HS and PMT) improved when local calibrations are performed (Gavilán et al. 2006; Paredes et al. 2018). These reduce the problem when wind speed and solar radiation are the major driving variables.

Studies in Spain comparing HS and PMT methodologies were studied in moist sub-humid climate zones
90 (Northern Spain) showing a better fit in PMT than in HS. (Lopez Moreno et al., 2009). Tomas -Burguera (2017) reported for the Iberian Peninsula a better adjustment of PMT than HS, provided that the lost values were filled by interpolation and not by estimation in the model of PMT.

Normally the calibration of models for ET_0 estimation is done from a spatial approach, calibrating models in the locations studied. Very few studies have been carried out to test models from the seasonal point of
95 view, being the annual calibration the most studied. Meanwhile spatial and annual approaches are of great interest for climatology and meteorology, for agriculture, seasonal or even monthly calibrations are relevant for crop (Nouri and Homae, 2018). To improve accuracy of ET_0 estimations, Paredes et al. 2018 used the values of the calibration constants values in the models were derived for October-March and April-September semesters.

100 The aim of this study was to evaluate the performance of temperature models for the estimation of reference evapotranspiration with a temporal (annual or seasonal) and spatial perspective in the Duero basin (Spain). The models evaluated were two Hargreaves-Samani (HS), with calibration and without calibration and five Penman- Monteith temperature model (PMT) analyzing the contribution of wind speed, humidity and solar radiation in a situation of limited agrometeorological data.

105

2. Materials and Method

2.1 Description of the Study Area

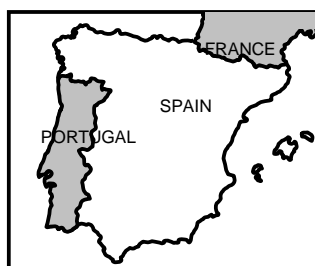
The study focuses on the Spanish part of the Duero hydrographic basin. The international hydrographic Duero basin is the most extensive of the Iberian Peninsula with 98073 km², it includes the territory of the
110 Duero river basin as well as the transitional waters of the Oporto Estuary and the associated Atlantic coastal ones (CHD, 2019). It is a shared territory between Portugal with 19214 km² (19.6 % of the total area) and Spain with 78859 km² (80.4%). The Duero river basin is located in Spain between the parallels 43° 5' N and 40° 10' N and the meridians 7° 4' W and 1° 50' W (Fig. 1). This basin is almost exactly



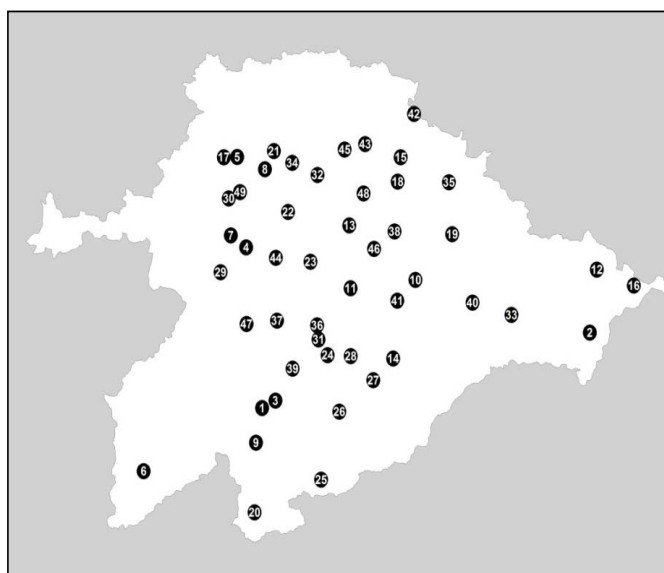
115 with the so-called *Submeseta Norte*, an area with an average altitude of 700 m, delimited by mountain
ranges with a much drier central zone that contains large aquifers, being the most important area of
agricultural production. The Duero Basin belongs in its 98.4% to the Autonomous Community of *Castilla*
y León. The 70% of the average annual precipitation is used directly by the vegetation or evaporated
from surface, this represents 35.000 hm³. The remaining (30%) is the total natural runoff. Mediterranean
is the predominant climate. The 90% of surface is affected by summer drought conditions. The average
120 annual values are: 12 °C of temperature and 612 mm of precipitation. However in precipitation there are
ranges with minimum values of 400 mm (South-Central area of the basin) and maximum of 1800 mm in
the northeast of the basin (CHD, 2019). According to Lautensach (1967), 30 mm is the threshold
definition of a dry month. Therefore, between 2 and 5 dry periods can be found in the basin (Ceballos et
al. 2004). Moreover, the climate variability, especially precipitation, exhibited in the last decade has
125 decreased the water availability for irrigation in this basin (Segovia- Cardozo et al. 2019).

The Duero basin has 4 million hectares of rainfed crops and some 500,000 hectares irrigated that
consumes 75% of the basin's water resources consumption. Barley (*Hordeum vulgare* L.) is the most
important rainfed crop in the basin occupying 36% of the National Crop Surface followed by wheat
(*Triticum aestivum* L.) with 30% (MAPAMA, 2019). Sunflower (*Helianthus annuus* L.) representing
130 30% of the National crop surface. This crop is mainly unirrigated (90%). Maize (*Zea mays* L.), alfalfa
(*Medicago sativa* L.) and sugar beet (*Beta vulgaris* L. var. *sacharifera*) are the main irrigated crops. These
crops representing 29 %, 30% and 68% of each National crop area, respectively. Finally, Vine (*Vitis*
vinifera L.) fills 72000 ha and irrigated less than 10%. For the irrigated crops of the basin there are water
allocations that fluctuate depending on the availability of water during the agricultural year and the type
135 of crop. These values fluctuate from 1200-1400 m³ / ha for vine up to 6400-7000 m³/ha for maize and
alfalfa. The use rates of the irrigation systems used in the basin are: 25 %, 68% and 7% for surface,
sprinkler and drip irrigation respectively (*Plan Hidrológico*, 2019).

140



145





150 Figure. 1. Location of study area. The point with the number indicates the location of the
agrometeorological stations according to Table 1.

2.2 Meteorological Data

Daily climate data were collected from 49 stations (Fig. 1B) from the agrometeorological network SIAR
155 (Irrigation Agroclimatic Information System; SIAR in Spanish language), which is managed by the
Spanish Ministry of Agriculture, Food and Environment (SIAR, 2018). The period studied was from
2000 to 2018, although the start date may fluctuate depending on the availability of data. Table 1 shows
the coordinates of the agrometeorological stations used in the Duero Basin and the aridity index based on
UNEP (1997). Table 1 the predominance of the semi-arid climate zone with 42 stations of the 49, being 2
160 arid, 4 dry-sub humid and 1 moist sub-humid.

Each station incorporate measurements of air temperature (T) and relative humidity (RH; Vaisala
HMP155), precipitation (ARG100 rain gauge), solar global radiation (pyranometer SKYE SP1110) and
wind direction and wind speed (U) (wind vane and RM YOUNG 05103 anemometer). Data were
recorded and averaged hourly on a data logger (Campbell CR10X and CR1000). Characteristics of the
165 agrometeorological stations were described by (Moratiel et al., 2011, 2013).

Table 1. Agrometeorological station used in the study. Coordinates and Aridity Index.

Stations	Latitude ⁽¹⁾	Longitude ⁽¹⁾	Altitude (m)	Aridity Index
1 Aldearrubia	40.99	-5.48	815	moist sub-humid
2 Almazán	41.46	-2.50	943	semi-arid
3 Arabayona	41.04	-5.36	847	semi-arid
4 Barcial del Barco	41.93	-5.67	738	semi-arid
5 Bustillo del Páramo	42.46	-5.77	874	semi-arid
6 Ciudad Rodrigo	40.59	-6.54	635	semi-arid
7 Colinas de Trasmonte	42.00	-5.81	709	semi-arid
8 Cubillas de los Oteros	42.40	-5.51	769	semi-arid
9 Ejeme	40.78	-5.53	816	semi-arid
10 Encinas de Esgueva	41.77	-4.10	816	semi-arid
11 Finca Zamadueñas	41.71	-4.70	714	semi-arid
12 Fuentecantos	41.83	-2.43	1063	semi-arid
13 Fuentes de Nava	42.08	-4.72	744	semi-arid
14 Gomezserracín	41.30	-4.30	870	semi-arid
15 Herrera de Pisuerga	42.49	-4.25	821	semi-arid
16 Hinojosa del Campo	41.73	-2.10	1043	semi-arid
17 Hospital de Orbigo	42.46	-5.90	835	semi-arid
18 Lantadilla	42.34	-4.28	798	semi-arid
19 Lerma	42.04	-3.77	840	semi-arid
20 Losar del Barco	40.37	-5.53	1024	semi-arid



21	Mansilla mayor	42.51	-5.43	791	semi-arid
22	Mayorga	42.15	-5.29	748	semi-arid
23	Medina de Rioseco	41.86	-5.07	739	semi-arid
24	Medina del Campo	41.31	-4.90	726	arid
25	Muñogalindo	40.58	-4.93	1128	arid
26	Nava de Arévalo	40.98	-4.78	921	semi-arid
27	Nava de la Asunción	41.17	-4.48	822	semi-arid
28	Olmedo	41.31	-4.69	750	semi-arid
29	Pozuelo de Tábara	41.78	-5.90	714	semi-arid
30	Quintana del Marco	42.22	-5.84	750	semi-arid
31	Rueda	41.40	-4.98	709	semi-arid
32	Sahagún	42.37	-5.02	856	semi-arid
33	San Esteban de Gormaz	41.56	-3.22	855	semi-arid
34	Santas Martas	42.44	-5.26	885	semi-arid
35	Tardajos	42.35	-3.80	770	dry sub-humid
36	Tordesillas	41.49	-5.00	658	semi-arid
37	Toro	41.51	-5.37	650	semi-arid
38	Torquemada	42.05	-4.30	868	semi-arid
39	Torrecilla de la Orden	41.23	-5.21	793	semi-arid
40	Vadocondes	41.64	-3.58	870	semi-arid
41	Valbuena de Duero	41.64	-4.27	756	semi-arid
42	Valle de Valdelucio	42.75	-4.13	975	dry sub-humid
43	Villaeles de Valdavia	42.56	-4.59	885	semi-arid
44	Villalpando	41.88	-5.39	701	semi-arid
45	Villaluenga de la Vega	42.53	-4.77	927	dry sub-humid
46	Villamuriel de Cerrato	41.95	-4.49	750	dry sub-humid
47	Villalarbo	41.48	-5.64	659	semi-arid
48	Villoldo	42.27	-4.59	817	semi-arid
49	Zotes del Páramo	42.26	-5.74	779	semi-arid

⁽¹⁾ Degrees

170

2.3 Estimates of Reference Evapotranspiration

2.3.1 FAO Penman-Monteith (FAO-PM)

FAO recommend the PM method as the one for computing ET_0 and evaluating other ET_0 models like Penman-Monteith model using only temperature data (PMT) or other temperature-based model (Allen et al. 1998). The method estimates the potential evapotranspiration from a hypothetical crop with an assumed height of 0.12 m having aerodynamic resistance of $(r_a) 208/u_2$, (u_2 is the mean daily wind speed measured at a 2 m height over the grass) and a surface resistance (r_s) of $70 \text{ s} \cdot \text{m}^{-1}$ and an albedo of 0.23, closely resembling the evaporation of an extension surface of green grass of uniform height, actively growing and adequately watered. The ET_0 ($\text{mm} \cdot \text{d}^{-1}$) was estimated following FAO-56 (Allen et al. 1998):

180



$$ET_o = \frac{0.408 \Delta (R_n - G) + \gamma \frac{900}{T + 273} u_2 (e_s - e_a)}{\Delta + \gamma(1 + 0.34u_2)} \quad [1]$$

In Eq. 1, R_n is net radiation at the surface ($\text{MJ m}^{-2} \text{d}^{-1}$), G is ground heat flux density ($\text{MJ m}^{-2} \text{d}^{-1}$), γ is the psychrometric constant ($\text{kPa } ^\circ\text{C}^{-1}$), T is mean daily air temperature at 2 m height ($^\circ\text{C}$), u_2 is wind speed at 2 m height (m s^{-1}), e_s is the saturation vapor pressure (kPa), e_a is the actual vapor pressure (kPa) and Δ is the slope of the saturation vapor pressure curve ($\text{kPa } ^\circ\text{C}^{-1}$), and. A stated Allen et al.(1998) setting G to zero is accepted in Eq.1.

2.3.2 Hargreaves-Samani (HS)

The scarce availability of agrometeorological data (global solar radiation, air humidity and wind speed mainly) limit the use of the PM-FAO method in many locations. Allen et al., (1998) recommended applying Hargreaves-Samani expression for situations where only the air temperature is available. The Hargreaves-Samani formulation (HS) is an empirical method that requires empirical coefficients calibrating (Hargreaves and Samani, 1982, 1985). The Hargreaves and Samani (Hargreaves and Samani, 1982, 1985) method is given by the following equation (2):

$$ET_o = 0.0135 \cdot k_{RS} \cdot 0.408 \cdot H_o \cdot (T_m + 17.8) \cdot (T_x - T_n)^{0.5} \quad (2)$$

where ET_o is the reference evapotranspiration (mm day^{-1}); H_o is extraterrestrial radiation ($\text{MJ} \cdot \text{m}^{-2} \cdot \text{d}^{-1}$); k_{RS} is the Hargreaves empirical coefficient, T_m , T_x and T_n are the daily mean, maximum and minimum air temperature ($^\circ\text{C}$), respectively. The value k_{RS} was initially set to 0.17 for arid and semiarid regions (Hargreaves and Samani, 1985). Hargreaves (1994) later recommended to use the value of 0.16 for interior regions and 0.19 for coastal regions. Daily temperature variations can occur due to other factors as topography, vegetation, humidity, among others, thus contemplating a fixed coefficient may lead to errors. In this study, we use the 0.17 as original coefficient (HS_o) and the calibrated coefficient k_{RS} (HS_c).The k_{RS} reduces the inaccuracy and consequently thus improving the estimation of ET_o . This calibration was done for each station.

2.3.3 Penman- Monteith Temperature (PMT)

The PM-FAO, when applied using only measured temperature data is denominated to as Penman-Monteith Temperature (PMT) retains many of the dynamics of the full data PM-FAO (Pereira et al., 2015; Hargreaves and Allen, 2003). The first reference of the use of PMT for limited meteorological data was Allen (1995), subsequently, studies like those of Allen et al. (1996), Annandale et al. (2002), were carried out with similar behavior to HS and PM-FAO, although there was the disadvantage of a greater preparation and computation of the data than the HS method. On this point, it should be noticed that the researchers do not favor to using PMT formulation and adopting the HS equation, simpler and easier to use (Paredes et al., 2018). Today, PMT calculation process is easily implemented with the new computers (Quej et al., 2019).

Wind speed, humidity and solar radiation are estimated in the PMT model using only air temperature as input for the calculation of ET_o . In this model, where global solar radiation (or sunshine data) is lacking,



the difference between the maximum and minimum temperature can be used, as an indicator of
 215 cloudiness and atmospheric transmittance, for the estimation of solar radiation [Eq.3] (Hargreaves and
 Samani, 1982). Net solar shortwave and longwave radiation estimates are obtained as indicated by Allen
 et al., (1998), equation 4 and 5 respectively. The expression of PMT is obtained as indicated in equations
 4, 5, 6, 7 and 8.

$$220 \quad R_s = H_o \cdot k_{RS} \cdot (T_x - T_n)^{0.5} \quad (3)$$

$$R_{ns} = 0.77 \cdot H_o \cdot k_{RS} \cdot (T_x - T_n)^{0.5} \quad (4)$$

where R_s is solar radiation ($\text{MJ} \cdot \text{m}^{-2} \cdot \text{d}^{-1}$); R_{ns} is net solar shortwave radiation ($\text{MJ} \cdot \text{m}^{-2} \cdot \text{d}^{-1}$); H_o is
 extraterrestrial radiation ($\text{MJ} \cdot \text{m}^{-2} \cdot \text{d}^{-1}$); H_o was computed as a function of site latitude, and solar angle and
 the day of the year Allen et al. (1998). T_x is daily maximum air temperature ($^{\circ}\text{C}$), T_n is daily minimum air
 225 temperature ($^{\circ}\text{C}$). For k_{RS} Hargreaves (1994) recommended to use $k_{RS} = 0.16$ for interior regions and k_{RS}
 = 0.19 for coastal regions. For better accuracy the coefficient k_{RS} can be adjusted locally (Hargreaves and
 Allen 2003). In this study two assumptions of k_{RS} were made, one where a value of 0.17 was fixed and
 another where it was calibrated for each station.

$$R_{nl} = 1.35 \cdot \left(\frac{k_{RS} \cdot (T_x - T_n)^{0.5}}{0.75 - 2z \cdot 10^{-5}} \right) \cdot \left(0.34 - 0.14 \left(0.6108 \cdot \exp \left(\frac{17.27 \cdot T_d}{T_d - 237.3} \right) \right)^{0.5} \right) \cdot \sigma$$

$$\cdot \left(\frac{(T_x + 273.15)^4 + (T_n + 273.15)^4}{2} \right) \quad (5)$$

Where R_{nl} is net longwave radiation ($\text{MJ} \cdot \text{m}^{-2} \cdot \text{d}^{-1}$) T_x is daily maximum air temperature ($^{\circ}\text{C}$); T_n is daily
 230 minimum air temperature ($^{\circ}\text{C}$); T_d is dew point temperature ($^{\circ}\text{C}$) calculated with the T_n according to
 Todorovic et al., 2013; σ Stefan-Boltzmann constant for a day ($4.903 \cdot 10^{-9} \text{ MJK}^{-4} \text{ m}^{-2} \text{ d}^{-1}$); z is the
 altitude (m).

$$PMT_{rad} = \left(\frac{0.408\Delta}{\Delta + \gamma(1 + 0.34u_2)} \right) \cdot (R_{ns} - R_{nl} - G) \quad (6)$$

$$PMT_{aero} = \frac{\gamma \cdot \frac{900 \cdot u_2}{T_m + 273} \cdot \left(\frac{e_{s(T_x)} + e_{s(T_n)}}{2} \right) - e_{s(T_d)}}{\Delta + \gamma(1 + 0.34u_2)} \quad (7)$$

$$PMT = PMT_{rad} + PMT_{aero} \quad (8)$$

Where PMT is the reference evapotranspiration estimate by Penman-Montheit temperature method
 ($\text{mm} \cdot \text{d}^{-1}$); PMT_{rad} is the radiative component of PMT ($\text{mm} \cdot \text{d}^{-1}$); PMT_{aero} is the aerodynamic component of
 235 PMT ($\text{mm} \cdot \text{d}^{-1}$); Δ is the slope of the saturation vapor pressure curve ($\text{kPa } ^{\circ}\text{C}^{-1}$), γ is the psychrometric
 constant ($\text{kPa } ^{\circ}\text{C}^{-1}$), R_{ns} is net solar shortwave radiation ($\text{MJ m}^{-2} \text{d}^{-1}$), R_{nl} is net longwave radiation (MJ
 $\text{m}^{-2} \text{d}^{-1}$), G is ground heat flux density ($\text{MJ m}^{-2} \text{d}^{-1}$) considered zero according to Allen et al.1998, T_m is
 mean daily air temperature ($^{\circ}\text{C}$), T_x is maximum daily air temperature, T_n is mean daily air temperature,
 T_d is dew point temperature ($^{\circ}\text{C}$) calculated with the T_n according to Todorovic et al. (2013), u_2 is wind



240 speed at 2 m height ($m s^{-1}$) and e_s is the saturation vapor pressure (kPa). In this model two assumptions of
 k_{RS} were done, one where a value of 0.17 was fixed and another where it was calibrated for each station.

2.3.4 Calibration and models

We studied two methods to estimate the ETo: Hargreaves–Samani (HS) and reference
 245 evapotranspiration estimate by Penman-Montheit temperature (PMT). Within these methods, different
 adjustments are proposed based on the adjustment coefficients of the methods and the missing data. The
 parametric calibration for the 49 stations was applied in this study. In order to decrease the errors of the
 evapotranspiration estimates, local calibration was used. The seven methods used with the coefficient
 250 (k_{RS}) of the calibrated and characteristics in the different locations studied are showed in Table 2. The
 calibration of the model coefficients was achieved by the nonlinear least squares fitting technique. The
 analyzed were calculated on yearly and seasonal bases. The seasons were the following: (1) winter
 (December, January, and February or DJF), (2) spring (March, April, and May or MAM), (3) summer
 (June, July, and August or JJA), (4) autumn (September, October, and November or SON).

255 Table 2. Characteristics of the models used in this study.

Model	Coefficient K_{RS}	u_2 (m/s)	Td (°C)
HS _O	0.17	-	-
HS _C	Calibrated	-	-
PMT _{O2T}	0.17	2	Todorovic ⁽¹⁾
PMT _{C2T}	Calibrated	2	Todorovic ⁽¹⁾
PMT _{OUT}	0.17	Average ⁽²⁾	Todorovic ⁽¹⁾
PMT _{OUH}	0.17	Average ⁽²⁾	Average ⁽³⁾
PMT _{CUH}	Calibrated	Average ⁽²⁾	Average ⁽³⁾

⁽¹⁾Dew point temperature obtained according to Todorovic et al. (2013).

⁽²⁾Average monthly value of wind speed

⁽³⁾Average monthly value of maximum and minimum relative humidity.

260 2.4. Performance assessment.

Model's suitability, accuracy and performance were evaluated using coefficient of determination (R^2 ; Eq.
 [9]) of the n pairs of observed (O_i) and predicted (P_i) values. Also, the mean absolute error (MAE, $mm \cdot d^{-1}$;
 Eq. [10]), root mean square error (RMSE; Eq. [11]) and The Nash-Sutcliffe model efficiency
 coefficient (NSE; Eq. [12]) (Nash and Sutcliffe 1970) was used. The coefficient of regression line (b),
 265 forced through the origin, is obtained by predicted values divided by observed values (ET_{model}/ET_{FAO56})
 The results were represented in a map applying of the Kriging method with the Surfer® 8 program.

$$R^2 = \left\{ \frac{\sum_{i=1}^n (O_i - \bar{O}) \cdot (P_i - \bar{P})}{\left[\sum_{i=1}^n (O_i - \bar{O})^2 \right]^{0.5} \cdot \left[\sum_{i=1}^n (P_i - \bar{P})^2 \right]^{0.5}} \right\}^2 \quad (9)$$



$$MAE = \frac{1}{n} \sum_{i=1}^n (|O_i - P_i|) \quad (\text{mm} \cdot \text{d}^{-1}) \quad (10)$$

$$RMSE = \left[\frac{\sum_{i=1}^n (O_i - P_i)^2}{n} \right]^{0.5} \quad (\text{mm} \cdot \text{d}^{-1}) \quad (11)$$

$$NSE = 1 - \left[\frac{\sum_{i=1}^n (O_i - P_i)^2}{\sum_{i=1}^n (O_i - \bar{O})^2} \right] \quad (12)$$

3. Results and Discussion

The Duero basin is characterized by being a semiarid climate zone (94% of the stations) according to Todorovic et al. (2013), where the P / ET_o ratio is between 0.2-0.5. The mean annual rainfall is 428 mm while the average annual ET_o for Duero basin is of 1079 mm, reaching the maximum values in the zone center-south with values that surpass slightly 1200 mm (Fig. 2). The great temporal heterogeneity is observed in the Duero Basin with values of 7% of the ET_o during the winter months (DJF) while during the summer months (JJA) they represent 47% of the annual ET_o . In addition, the months from May till September represent 68% of the annual ET_o , with similar values as reported by Moratiel et al. (2011).

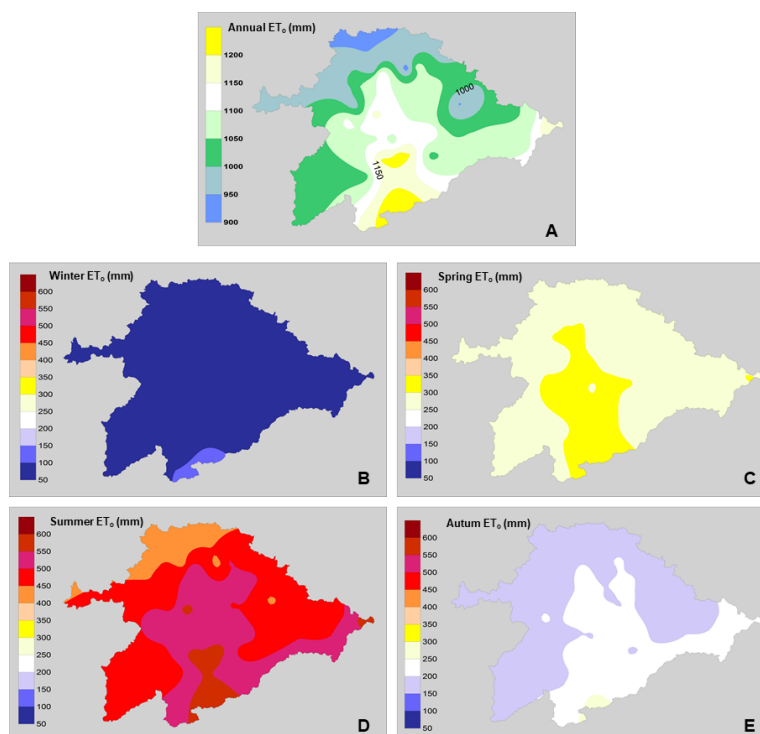


Figure.2. Mean values season of ET_o (mm) during the study period 2000-2018. A, annual; B, winter (December, January, and February or DJF); C, spring (March, April, and May or MAM); D, summer (June, July, and August or JJA) and E, autumn (September, October, and November or SON).



280

Table 3 shows the different statistics analyzed in the seven models studied as a function of the season of the year and annually. From an annual point of view all the models show R^2 values higher than 0.91, NSE higher than 0.88, MAE less than 0.52, RMSE lower than 0.69 and underestimates or overestimates of the models by $\pm 4\%$. The best behavior is shown by the PMT_{CHU} model with MAE and RMSE of $0.39 \text{ mm}\cdot\text{d}^{-1}$ and $0.52 \text{ mm}\cdot\text{d}^{-1}$ respectively. PMT_{CHU} shows no tendency with a coefficient of regression b of 1.0. The Values of NSE and R^2 are 0.93. The models HSc and PMT_{OUH} have a similar behavior with same MAE ($0.41 \text{ mm}\cdot\text{d}^{-1}$), NSE (0.92) and R^2 (0.91). RMSE is 0.55 for PMT_{OUH} model and $0.54 \text{ mm}\cdot\text{d}^{-1}$ for HSc model. The models PMT_{OUT} and HSO showed a slightly higher performance than the models that worse statistical data showed PMT_{O2T} and PMT_{C2T} (Fig.3). Respect to the models, it can be seen how their performance improves as the averages of wind speed (u) and dew temperature (T_d) values are incorporated. The same pattern is shown between the PMT_{CUH} models, where the mean u values and T_d are incorporated, and PMT_{C2T} , with u of 2 m/s and dew temperature with the approximation of Todorovic et al. (2013). These adjustments are supported because the adiabatic component of evapotranspiration in the PMT equation is very influential in the Mediterranean climate, especially wind speed (Moratiel et al., 2010). In addition, trends and fluctuations of u have been reported as the factor that most influences ETo trends (Nouri et al., 2017, McVicar et al., 2012; Moratiel et al., 2011). Moreover, errors in the estimation of relative humidity cause substantial changes in the estimation of ETo as reported by Nouri and Homae (2018) and Landaras et al. (2008).

285

290

295

300

305

Jobloun and Sahli (2008) cited RMSE of $0.41\text{-}0.80 \text{ mm}\cdot\text{d}^{-1}$ for Tunisia. The authors showed for the PMT model better performance than for the Hargreaves non calibrated model. Raziei and Pereira (2013) reported data of RMSE for semiarid zone in Iran between 0.27 and $0.81 \text{ mm}\cdot\text{d}^{-1}$ for HSc model and 0.30 and $0.79 \text{ mm}\cdot\text{d}^{-1}$ for PMT_{C2T} , although these authors use monthly averages in their models. Ren et al. (2016) reported values of RMSE in a range of 0.51 to $0.90 \text{ mm}\cdot\text{d}^{-1}$ for PMT_{C2T} and range of 0.81 to $0.94 \text{ mm}\cdot\text{d}^{-1}$ for HSc in semiarid locations in Inner Mongolia (China). Todorovic et al. (2013) found that the PMT_{O2T} method have better performance than the uncalibrated HS method (HSO), with RMSE average of $0.47 \text{ mm}\cdot\text{d}^{-1}$ for PMT_{O2T} and 0.52 HSO. At this point, we should highlight that in our study daily values data have been used.

From a spatial perspective, it is observed in Fig. 3 that the areas where the values of MAE are higher are to the east and southwest of the basin. This is due to the fact that the average wind speed in the eastern zone is higher than 2.5 m/s, for example, the Hinojosa del Campo station shows average annual values of 3.5 m/s. The southwest area shows values of wind speeds below 1.5 m/s as the Ciudad Rodrigo station with annual average values of 1.19 m/s.

310

315



320 Table 3. Statistical indicators for ET_o estimation in the seven models studied for different season. Average data for the 49 stations studied.

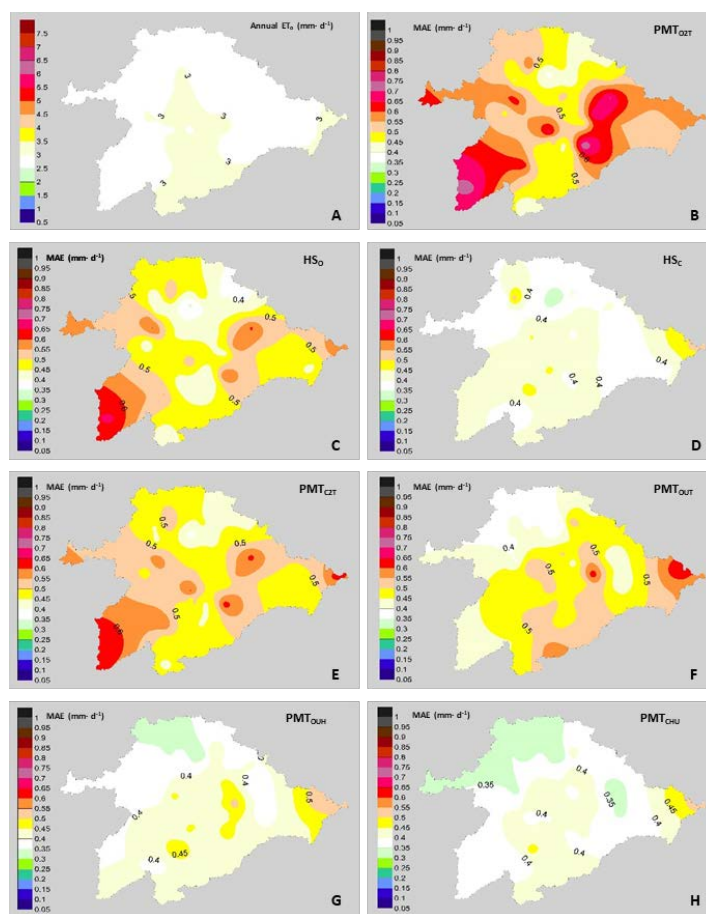
Season	Variable	MODEL							Daily Average (ETFAO5 ₆ , mm·d ⁻¹)
		HS _O	HS _C	PMT _{O2T}	PMT _{C2T}	PMT _{OUT}	PMT _{OUH}	PMT _{CUH}	
Annual	R ²	0.93	0.93	0.91	0.91	0.92	0.93	0.93	2.95
	NSE	0.90	0.92	0.88	0.89	0.90	0.92	0.93	
	MAE (mm·d ⁻¹)	0.47	0.41	0.52	0.50	0.47	0.41	0.39	
	RMSE(mm·d ⁻¹)	0.62	0.54	0.69	0.66	0.62	0.55	0.52	
	b	1.03	0.97	1.04	1.02	1.03	1.03	1.00	
Winter (DJF)	R ²	0.53	0.53	0.56	0.55	0.56	0.59	0.59	0.90
	NSE	0.43	0.50	0.36	0.35	0.35	0.57	0.58	
	MAE (mm·d ⁻¹)	0.27	0.25	0.29	0.30	0.30	0.24	0.24	
	RMSE(mm·d ⁻¹)	0.35	0.33	0.36	0.37	0.37	0.30	0.30	
	b	0.99	0.93	1.07	1.06	1.09	0.96	0.96	
Spring (MAM)	R ²	0.83	0.83	0.81	0.81	0.81	0.82	0.82	3.19
	NSE	0.80	0.81	0.75	0.78	0.74	0.80	0.81	
	MAE (mm·d ⁻¹)	0.43	0.42	0.50	0.46	0.52	0.45	0.43	
	RMSE(mm·d ⁻¹)	0.56	0.55	0.62	0.59	0.65	0.57	0.55	
	b	1.01	0.95	1.04	1.00	1.06	1.02	0.99	
Summer (JJA)	R ²	0.59	0.59	0.53	0.53	0.56	0.60	0.60	5.48
	NSE	0.32	0.54	0.21	0.31	0.45	0.52	0.59	
	MAE (mm·d ⁻¹)	0.68	0.56	0.72	0.68	0.62	0.57	0.53	
	RMSE(mm·d ⁻¹)	0.84	0.71	0.91	0.87	0.79	0.73	0.68	
	b	1.04	0.98	1.03	1.00	1.00	1.03	1.00	
Autumn (SON)	R ²	0.85	0.85	0.83	0.83	0.84	0.86	0.86	2.21
	NSE	0.72	0.82	0.61	0.65	0.78	0.83	0.85	
	MAE (mm·d ⁻¹)	0.50	0.40	0.58	0.55	0.46	0.40	0.38	
	RMSE(mm·d ⁻¹)	0.62	0.52	0.73	0.70	0.58	0.51	0.49	
	b	1.09	1.02	1.14	1.12	1.07	1.05	1.02	

325 These MAE differences are more pronounced in those models in which the average wind speed is not taken, such as the PMT_{C2T} and PMT_{O2T} models. Most of the basin takes values of wind speeds between 1.5 and 2.5 m/s. The lower MAE values in the northern zone of the basin are due to the lower average values of DPV than the central area, with values of 0.7 kPa in the northern zone and 0.95 kPa in the central zone. Same trends in the effect of wind on the ET_o estimates were detected by Nouri and Homae (2018) where they indicated that values outside the range of 1.5-2.5 m/s in models where the default u



was set at 2 m / s , increased the error of the ETo. Even models such as HS, where the influence of the
wind speed values are not directly indicated outside the ranges previously mentioned, their performance is
330 not good and some authors have proposed HS calibrations based on wind speeds in Spanish basins such
as the Ebro Basin (Martinez-Cob and Tejero-Juste, 2004). In our study, the HSc model showed good
performance with MAE values similar to PMT_{CUH} and PMT_{OUH} (Fig.3).

The performance of the models by season of the year changes considerably, obtaining lower adjustments
with values of R^2 0.53 for winter (DJF) in the models of HSo and HSc and for summer (JJA) in the
335 models PMT_{O2T} and PMT_{C2T} . All models during spring and autumn show R^2 above 0.8. The NSE for
models HSo, PMT_{C2T} , PMT_{O2T} and PMT_{OUT} in summer and winter are at unsatisfactory values below 0.5
(Moriassi et al. 2007). The mean values (49 stations) of MAE and RMSE for the models in the winter were
0.24 -0.30 $\text{mm}\cdot\text{d}^{-1}$ and 0.3-0.37 $\text{mm}\cdot\text{d}^{-1}$ respectively. For spring, the ranges were between 0.42-0.52
340 $\text{mm}\cdot\text{d}^{-1}$ for MAE and 0.55-0.65 $\text{mm}\cdot\text{d}^{-1}$ for RMSE. In summer, MAE fluctuated between 0.53-0.72 $\text{mm}\cdot\text{d}^{-1}$
and RMSE 0.68-0.91 $\text{mm}\cdot\text{d}^{-1}$. Finally, in autumn, the values of MAE and RMSE were 0.38-0.58 and
0.49-0.70 $\text{mm}\cdot\text{d}^{-1}$ respectively (Table 3). Very few studies, as far as we know, have been carried out of
adjustments of evapotranspiration models from a temporal point of view and generally the models are
usually calibrated and adjusted from an annual point of view. Some authors, such as Aguilar and Polo
(2011), differentiate seasons as wet and dry, others such as Paredes et al. (2018) divide in summer and
345 winter, Vangelis et al. (2013) take into account two periods and Nouri and Homae (2018) do it from a
monthly point of view. In most cases, the results obtained in these studies are not comparable with those
performed in this, since the time scales are different. However, it can be indicated that the results of the
models according to the time scale season differ greatly with respect to the annual scale.



350

Figure 3. Performance of the models with an annual focus. A, Average annual values of ET_0 ($mm \cdot d^{-1}$). Mean values of MAE ($mm \cdot d^{-1}$): B, PMT_{O2T} model; C, H_O model; D, H_C model; E, PMT_{C2T} model; F, PMT_{OUT} model; G, PMT_{OUH} model and H, PMT_{CUH} model

355

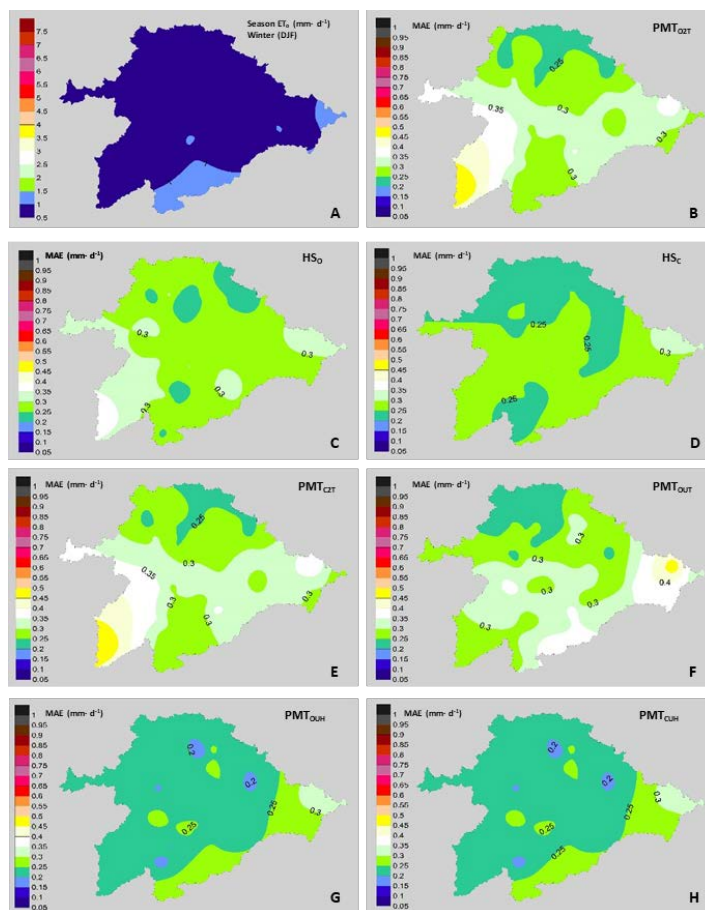


Figure 4. Performance of the models with a winter focus (December, January and February). A, Average values of ET_0 (mm·d⁻¹) in winter. Mean values of MAE (mm·d⁻¹): B, PMT_{C2T} model ;C, H₀ model; D, H_C model; E, PMT_{C2T} model; F, PMT_{OUT} model; G, PMT_{OUH} model and H, PMT_{CUH} model

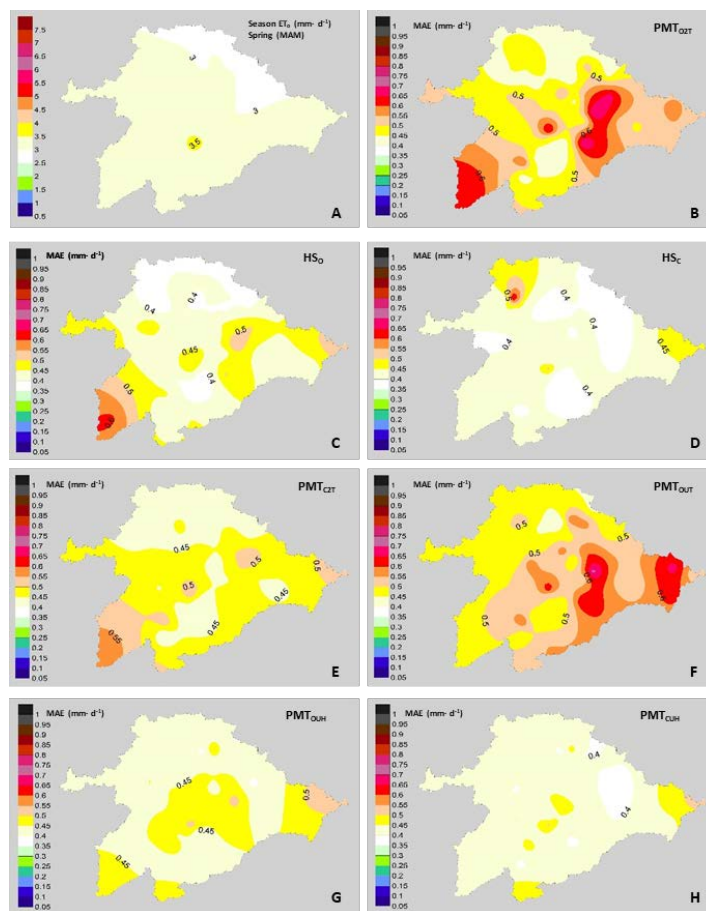


Fig.5. Performance of the models with a spring focus (March, April and May). A, Average annual values of ET_0 ($mm \cdot d^{-1}$) in spring. Mean values of MAE ($mm \cdot d^{-1}$): B, PMT_{O2T} model ;C, H_S model; D, H_C model; E, PMT_{C2T} model; F, PMT_{OUT} model; G, PMT_{OUH} model and H, PMT_{CUH} model

The model that shows the best performance independently of the seasonal is the PMT_{CUH} . The models that can be considered in a second step are the H_S and the PMT_{OUH} being the performance slightly better in the H_S model during the season of more solar radiation (spring and summer). The following models are below the aforementioned (PMT_{OUH} and H_S), being the one with the worst performance of the PMT_{O2T} model. Numerous authors have recommended to include, as much as possible, average data of local wind speeds for the improvement of the models as Nouri and Homae (2018) and Raziei and Pereira (2013) in Iran, Paredes et al. (2018) in Azores islands (Portugal), Djaman et al. (2017) in Uganda, Rojas and Sheffield (2013) in Louisiana (USA), Jabloun and Shali (2008) in Tunisia and Martinez-Cob and Tejero-Juste (2004) in Spain, among others. It is important to note that the PMT_{OUT} generally has a better performance than the PMT_{C2T} except for spring. The difference between both models is that in the



380 PMT_{C2T} k_{RS} is calibrated with wind speed set at 2 m/s and in the PMT_{OUT} k_{RS} is not calibrated and with an average wind. In this case the wind speed variable affects less than the calibration of k_{RS} since the average values of wind during spring (2.3 m/s) is very close to 2 m/s and there is no great variation between both settings. In this way, k_{RS} calibration shows a greater contribution than the average of the wind speed to improve the model (Fig.5 E, F).

385 The northern area of the basin is the area in which lower MAE shows in most models and for all seasons. This is due in part to the fact that the lower values of ET_o ($mm \cdot d^{-1}$) are located in the northern zone. On the other hand, the eastern zone of the basin shows the highest values of MAE error due to the strong winds that are located in that area.

During the winter the seven models tested show no great differences between them, although the PMT_{CUH} is the model with the best performance. It is important to indicate that during this season the RMSE (%) is placed in all the models above 30%, so they can be considered as very weak models. According to 390 Jamieson et al. (1991) and Bannayan and Hoogenboom (2009) the model is considered excellent with a normalized RMSE (%) less than 10%, good if the normalized RMSE (%) is greater than 10 and less than 20%, fair if the normalized RMSE (%) is greater than 20% and less than 30%, and poor if the normalized RMSE (%) is greater than 30%. All models that are made during the spring season (MAM) can be considered as good / fair since their RMSE (%) fluctuates between 17-20%. The seven models that are 395 made during summer season (JJA) can be considered as good since their RMSE varies from 12 to 16%. Finally, the models that are made during autumn (SON) are considered fair / poor fluctuating between the values of 22-32%. The models that reached values greater than 30% during autumn were the model PMT_{C2T} (31%) and PMT_{O2T} (32%) also with a clear tendency to overestimation (Table 3) Similar results were obtained in Iran by Nouri and Homaee (2018), where the months of December-January and 400 February the performance of the PMT and HS models tested had RMSE (%) values above 30%. In the use of temperature models for estimating ET_o , it is necessary to know the objective that is set. For the management of irrigation in crops is better to test the models in the period in which the species require the contribution of additional water. In many cases applying the models with an annual perspective with a good performance can lead to more accentuated errors in the period of greater water needs. The studies of 405 different temporal and spatial scales of the temperature models for ET_o estimation, can give information very close to the reality that allow to manage the water planning in zones where the economic development does not allow the implementation of agrometeorological stations due to its high cost.

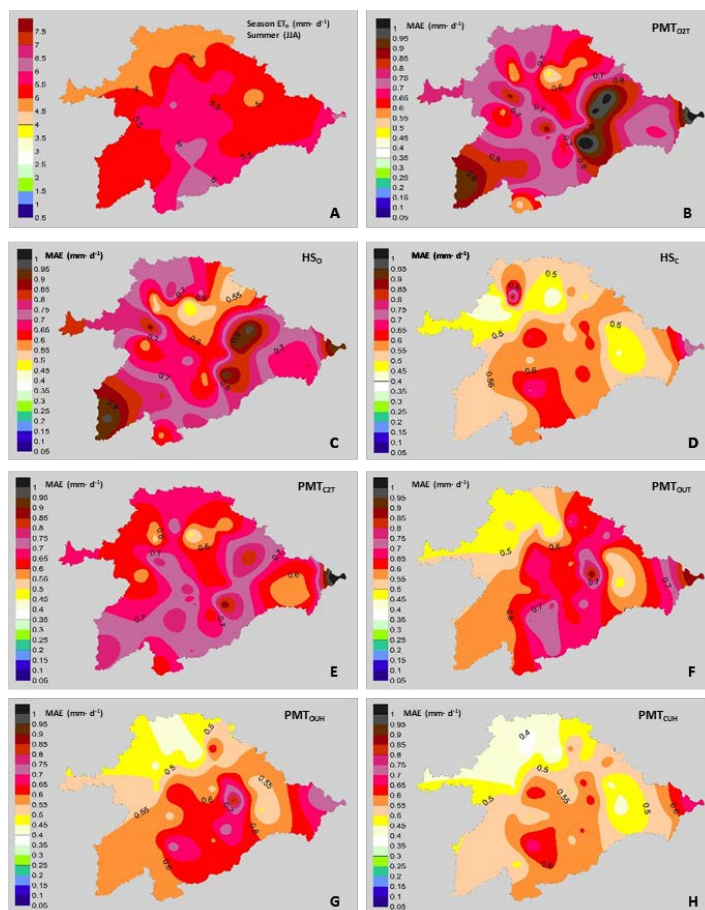


Fig.6. Performance of the models with a summer focus (June, July and August). A. Average values of ET_0 ($mm \cdot d^{-1}$) in summer. Mean values of MAE ($mm \cdot d^{-1}$): B, PMT_{O2T} model ;C, H_O model; D, H_C model; 410 E, PMT_{C2T} model; F, PMT_{OUT} model; G, PMT_{OUH} model and H, PMT_{CUH} model

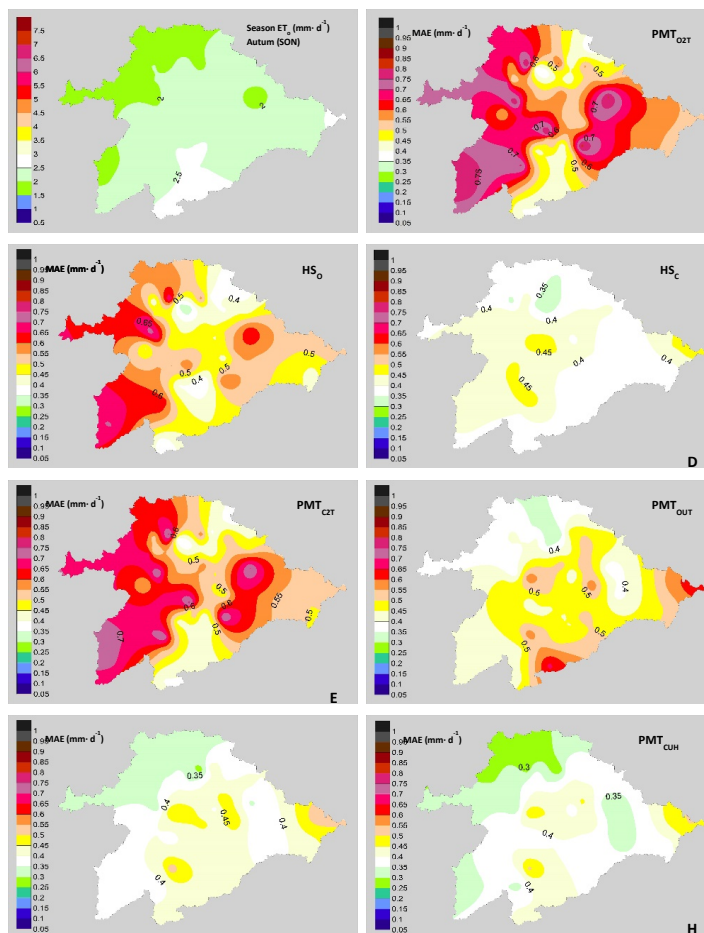


Fig.7. Performance of the models with an autumn focus (September, October and November). A. Average values of ET_0 ($mm \cdot d^{-1}$) in autumn. Mean values of MAE ($mm \cdot d^{-1}$): B, PMT_{O2T} model ;C, H_O model; D, H_C model; E, PMT_{C2T} model; F, PMT_{OUT} model; G, PMT_{OUH} model and H, PMT_{CUH} model

4. Conclusions

The performance of seven temperature-based models (PMT and HS) were evaluated in the Duero basin (Spain) with a total of 49 agrometeorological stations. Our studies revealed that the models tested on an annual or seasonal basis provide different performance. The values of R^2 are higher when they are performed annually with values between 0.91-0.93 for the seven models, but when performed from a seasonal perspective there are values that fluctuate between 0.5-0.6 for summer or winter and 0.86-0.81 for spring and autumn. The NSE values are high for models tested from an annual view, but for the seasons of spring and summer they are in values below 0.5 for the models H_S_O , PMT_{O2T} , PMT_{C2T} and PMT_{OUT} . The fluctuations between models with annual perspective of RMSE and MAE were greater than if those models were compared with a seasonal perspective. During the winter none of the models showed a good performance with values of $R^2 > 0.59$ $NSE > 0.58$ and $RMSE (\%) > 30\%$. From a practical point of view in the management of irrigated crops, winter is a season that does not worry too much in the use of



430 water in the basin since the daily average values are around 1 mm per day due to low temperatures,
radiation and DPV. The model that showed the best performance was PMT_{CUH} followed by PMT_{OUH} and
435 HS_C for annual and season criteria. PMT_{OUH} is slightly less robust than PMT_{CUH} during the maximum
radiations periods of spring and summer since the PMT_{CHU} performs the k_{RS} calibration. The performance
of the HS_C model is better in the spring period, which is similar to PMT_{CHU} . The spatial distribution of
MAE errors in the basin shows that it is highly dependent on wind speeds, obtaining greater errors in
440 areas with winds greater than 2.8 m/s (east of the basin) and lower than 1.3 m/s (south-southwest of the
basin). This information of the tested models in different temporal and spatial scales can be very useful to
adopt appropriate measures for an efficient water management under limitation of agrometeorological
data and under the recent increments of dry periods in this basin.

440 5. Acknowledgements

Financial support provided by MINECO (Ministerio de Economía y Competitividad) through project
PRECISOST (AGL2016-77282-C3-2-R) and project AGRISOST-CM (S2018/BAA-4330) is greatly
appreciated.

445 6. References

- Aguilar, C., and Polo, M.J.: Generating reference evapotranspiration surfaces from the Hargreaves
equation at watershed scale. *Hydrol. Earth Syst. Sci.*, 15, 2495–2508. <https://doi.org/10.5194/hess-15-2495-2011>. 2011
- 450 Allen, R. G.: Evaluation of procedures for estimating grass reference evapotranspiration using air
temperature data only. Report submitted to Water Resources Development and Management Service,
Land and Water Development Division, United Nations Food and Agriculture Service, Rome, Italy. 1995
- Allen, R. G.: Assessing integrity of weather data for use in reference evapotranspiration estimation. *J.*
Irrig. Drain. Eng., 122, 97–106, [https://doi.org/10.1061/\(ASCE\)0733-9437\(1996\)122:2\(97\)](https://doi.org/10.1061/(ASCE)0733-9437(1996)122:2(97)), 1996.
- 455 Allen, R.G., Pereira, L. S., Howell, T. A., and Jensen, E.: Evapotranspiration information reporting: I.
Factors governing measurement accuracy, *Agr. Water Manage.*, 98, 899-920,
<https://doi.org/10.1016/j.agwat.2010.12.015>, 2011.
- Allen, R. G., Pereira, L. S., Raes, D., and Smith, M.: Crops evapotranspiration, Guidelines for computing
crop requirements, Irrigations and Drainage Paper 56, FAO, Rome, 300 pp., 1998.
- 460 Almorox, J., Quej, V.H., and Martí, P.: Global performance ranking of temperature-based approaches for
evapotranspiration estimation considering Köppen climate classes, *J. Hydrol.*, 528, 514-522.
<http://dx.doi.org/10.1016/j.jhydrol.2015.06.057>. 2015.
- Annandale, J., Jovanovic, N., Benade, N., and Allen, R.G.: Software for missing data error analysis of
Penman-Monteith reference evapotranspiration. *Irrig. Sci.* 21, 57–67,
465 <https://doi.org/10.1007/s002710100047>, 2002.
- Bannayan, M., Hoogenboom, G.: Using pattern recognition for estimating cultivar coefficients of a crop
simulation model, *Field Crop Res.*, 111, 290-302. <https://doi.org/10.1016/j.fcr.2009.01.007>. 2009.



- Ceballos, A., Martínez-Fernández, J., and Luengo-Ugidos, M. A.: Analysis of rainfall trend and dry periods on a pluviometric gradient representative of Mediterranean climate in Duero Basin, Spain, J. Arid. Environ., 58, 215–233, <https://doi.org/10.1016/j.jaridenv.2003.07.002>, 2004.
- 470 Djaman, K., Rudnick, D., Mel, V.C., Mutiibwa, D., Diop, L., Sall, M., Kabenge, I., Bodian, A., Tabari, H., Irmak, S.: Evaluation of Valiantzas' simplified forms of the FAO-56 Penman-Monteith reference evapotranspiration model in a humid climate. J. Irr. Drain. Eng., 143, 06017005, [https://doi.org/10.1061/\(ASCE\)IR.1943-4774](https://doi.org/10.1061/(ASCE)IR.1943-4774). 2017.
- 475 Droogers, P., and Allen, R.G.: Estimating reference evapotranspiration under inaccurate data conditions. Irrig. Drain. Syst., 16: 33–45, <https://doi.org/10.1023/A:1015508322413>, 2002.
- CHD, Confederación Hidrográfica del Duero: <http://www.chduero.es>, last access: 28 January 2019.
- Gavilán, P., Lorite, J.I., Tornero and Berengera, J.: Regional calibration of Hargreaves equation for estimating reference ET in a semiarid environment. Agric. Water Manag., 81: 257–281. <https://doi.org/10.1016/j.agwat.2005.05.001>, 2006.
- 480 Hargreaves, G.H.: Simplified coefficients for estimating monthly solar radiation in North America and Europe. Departmental Paper, Dept. of BioI. and Irrig. Engrg., Utah State Univ., Logan, Utah. 1994.
- Hargreaves, G.H., and Samani, Z.A.: Estimating potential evapotranspiration., J. Irrig. Drain. Div., 108(3): 225–230. 1982.
- 485 Hargreaves, G.H., and Samani, Z.A.: Reference crop evapotranspiration from ambient air temperature, Am. Soc. Agric. Eng. (Microfiche Collect. no. fiche no. 85-2517). 1985.
- Hargreaves, G.H., and Allen, R.G.: History and Evaluation of Hargreaves Evapotranspiration Equation, J. of Irrig. and Drain. Eng., 129: 53-63, [https://doi.org/10.1061/\(ASCE\)0733-9437\(2003\)129:1\(53\)](https://doi.org/10.1061/(ASCE)0733-9437(2003)129:1(53)), 2003.
- Jamieson, P.D., Porter, J.R., Wilson, D.R.: A test of the computer simulation model ARCWHEAT1 on wheat crops grown in New Zealand. Field Crop Res. 27, 337-350. [https://doi.org/10.1016/0378-4290\(91\)90040-3](https://doi.org/10.1016/0378-4290(91)90040-3).1991.
- 490 Jabloun, M. D., and A. Sahli.: Evaluation of FAO-56 methodology for estimating reference evapotranspiration using limited climatic data: Application to Tunisia, Agric. Water Manage., 95, 707–715. <https://doi.org/10.1016/j.agwat.2008.01.009>, 2008.
- 495 Landeras, G., Ortiz-Barredo, A., and López, J.J.: Comparison of artificial neural network models and empirical and semi-empirical equations for daily reference evapotranspiration estimation in the Basque Country (Northern Spain). Agric. Water Manage. 95: 553–565. <https://doi.org/10.1016/j.agwat.2007.12.011>. 2008.
- Lautensach, H.: Geografía de España y Portugal, Vicens Vivens, Barcelona, 814 pp., 1967 (in Spanish).
- 500 López-Moreno, J.I., Hess, T.M., and White, A.S.M.: Estimation of Reference Evapotranspiration in a Mountainous Mediterranean Site Using the Penman-Monteith Equation With Limited Meteorological Data. Pirineos JACA, 164, 7–31, <https://doi.org/10.3989/pirineos.2009.v164.27.2009>.
- MAPAMA, Ministerio de Agricultura Pesca y Alimentación, Anuario de estadística. <https://www.mapa.gob.es/es/estadistica/temas/publicaciones/anuario-de-estadistica/>, last access: 28 de March 2019.
- 505 Martínez, C.J., and Thepadia, M.: Estimating Reference Evapotranspiration with Minimum Data in Florida, J. Irrig. Drain. En., 136,494-501, [https://doi.org/10.1061/\(ASCE\)IR.1943-4774.0000214](https://doi.org/10.1061/(ASCE)IR.1943-4774.0000214), 2010.



- Martínez-Cob, A., and Tejero-Juste, M.: A wind-based qualitative calibration of the Hargreaves ET_o estimation equation in semiarid regions, *Agric. Water Manage.* 64(3): 251–264.
510 [https://doi.org/10.1016/S0378-3774\(03\)00199-9](https://doi.org/10.1016/S0378-3774(03)00199-9). 2004.
- McVicar, T.R., Roderick, M. L., Donohue, R.J., Li L.T., G.VanNiel, T., Thomas, A., Grieser, J., Jhajharia, D., Himri, Y., Mahowald, N.M., Mescherskaya, A.V., Kruger, A.C., Rehman, S., and Dinpashoh, Y.: Global review and synthesis of trends in observed terrestrial near-surface wind speeds: implications for evaporation. *J. Hydrol.* 416–417: 182–205. <https://doi.org/10.1016/j.jhydrol.2011.10.024>.
515 2012.
- Mendicino, G., and Senatore, A.: Regionalization of the Hargreaves Coefficient for the Assessment of Distributed Reference Evapotranspiration in Southern Italy, *J. Irrig. Drain. Eng.* 139, 349–62, DOI: 10.1061/(ASCE)IR.1943-4774.0000547, 2012.
- Moratiel, R., Duran, J. M., and Snyder, R.: Responses of reference evapotranspiration to changes in atmospheric humidity and air temperature in Spain, *Clim. Res.*, 44, 27–40, <https://doi.org/10.3354/cr00919>. 2010.
- Moratiel, R., Snyder, R.L., Durán, J.M. and Tarquis, A.M.: Trends in climatic variables and future reference evapotranspiration in Duero valley (Spain). *Nat. Hazards Earth Syst. Sci.* 11, 1795–1805. 2011. <https://doi.org/10.5194/nhess-11-1795-2011>, 2011.
- 525 Moratiel, R., Martínez-Cob, A., and Latorre, B.: Variation in the estimations of ET_o and crop water use due to the sensor accuracy of the meteorological variables. *Nat. Hazards Earth Syst. Sci.*, 13, 1401-1410, <https://doi.org/10.5194/nhess-13-1401-2013>, 2013.
- Moriyas, D. N., Arnold, J. G., Van Liew, M. W., Bingner, R. L., Harmel, R. D., and Veith T. L.: Model evaluation guidelines for systematic quantification of accuracy in watershed simulations, *T. ASABE*, 50, 885-900. doi: 10.13031/2013.23153. 2007.
- 530 Nash, J. E., and Sutcliffe, J. V: River flow forecasting through conceptual models. Part I—A discussion of principles, *J. Hydrol.* 10, 282–290, [https://doi.org/10.1016/0022-1694\(70\)90255-6](https://doi.org/10.1016/0022-1694(70)90255-6), 1970.
- Nouri, M., Homae, M., and Bannayan, M.: Quantitative trend, sensitivity and contribution analyses of reference evapotranspiration in some arid environments under climate change. *Water Resour. Manage.* 31 (7), 2207–2224. <https://doi.org/10.1007/s11269-017-1638-1>. 2017.
- 535 Nouri, M., and Homae, M.: On modeling reference crop evapotranspiration under lack of reliable data over Iran. *J. Hydrol.* 566, 705-718. <https://doi.org/10.1016/j.jhydrol.2018.09.037>. 2018
- Paredes, P., Fontes, J.C., Azevedo, E.B., and Pereira, L.S.: Daily reference crop evapotranspiration with reduced data sets in the humid environments of Azores islands using estimates of actual vapor pressure, solar radiation, and wind speed. 1134:1115–1133. *Theor. Appl. Climatol.* 134:1115–1133
540 <https://doi.org/10.1007/s00704-017-2329-9>. 2018.
- Pereira, L.S.: Water, Agriculture and Food: Challenges and Issues, *Water Resour. Manage.*, 31, 2985-2999. <https://doi.org/10.1007/s11269-017-1664-z>, 2017.
- Pereira, L.S., Allen, R.G., Smith, M., and Raes, D.: Crop evapotranspiration estimation with FAO56: Past and future, *Agr. Water Manage.*, 147, 4-20, <http://dx.doi.org/10.1016/j.agwat.2014.07.031>, 2015.
- 545 Plan Hidrológico, Plan Hidrológico de la parte española de la demarcación hidrográfica del Duero. 2015-2021. Anejo 5. Demandas de Agua.



- <http://www.chduero.es/Inicio/Planificaci%C3%B3n/Planhidrol%C3%B3gico20162021Vigente/PlanHidro1%C3%B3gico/tabid/734/Default.aspx>. last access: 18 February 2019.
- 550 Quej, V.H., Almorox, J., Arnaldo, A., and Moratiel, R.: Evaluation of Temperature-Based Methods for the Estimation of Reference Evapotranspiration in the Yucatán Peninsula, Mexico, *J. Hydrol. Eng.*, 24(2): 05018029, [https://doi.org/10.1061/\(ASCE\)HE.1943-5584.0001747](https://doi.org/10.1061/(ASCE)HE.1943-5584.0001747), 2019.
- Raziei, T., and Pereira, L.S.: Estimation of ETo with Hargreaves-Samani and FAO-PM temperature methods for a wide range of climates in Iran, *Agric. Water Manag.* 121, 1–18, <https://doi.org/10.1016/j.agwat.2012.12.019>, 2013.
- 555 Rojas, J.P., and Sheffield, R.E.: Evaluation of daily reference evapotranspiration methods as compared with the ASCE-EWRI Penman-Monteith equation using limited weather data in Northeast Louisiana. *J. Irr. Drain. Eng.*, 139, 285–292. [https://doi.org/10.1061/\(ASCE\)IR.1943-4774.0000523](https://doi.org/10.1061/(ASCE)IR.1943-4774.0000523). 2013.
- 560 Ren, X., Qu, Z., Martins, D.S., Paredes, P., and Pereira, L.S.: Daily Reference Evapotranspiration for Hyper-Arid to Moist Sub-Humid Climates in Inner Mongolia, China: I. Assessing Temperature Methods and Spatial Variability, *Water Resour. Manag.*, 30(11), 3769–3791, <http://link.springer.com/10.1007/s11269-016-1384-9>, 2015.
- SIAR, Sistema de información Agroclimática para el Regadío, <http://portal.mapama.gob.es/websiar/Inicio.aspx>, last access 2 June 2018.
- 565 Segovia-Cardozo, D.A., Rodríguez-Sinobas, L., and Zobelzu, S.: Water use efficiency of corn among the irrigation districts across the Duero river basin (Spain): Estimation of local crop coefficients by satellite images, *Agric. Water Mang.* 212, 241–251, <https://doi.org/10.1016/j.agwat.2018.08.042>, 2019.
- Todorovic, M., Karic, B., and Pereira, L.S.: Reference Evapotranspiration estimate with limited weather data across a range of Mediterranean climates, *J. Hydrol.* 481, 166–176. <http://dx.doi.org/10.1016/j.jhydrol.2012.12.034>, 2013.
- 570 Tomas-Burguera, M., Vicente-Serrano, S.M., Grimalt, M., and Beguería, S.: Accuracy of reference evapotranspiration (ETo) estimates under data scarcity scenarios in the Iberian Peninsula, *Agr. Water Manage.* 182, 103–116 <http://dx.doi.org/10.1016/j.agwat.2016.12.013>, 2017.
- 575 Trajkovic, S.: Temperature-based approaches for estimating reference evapotranspiration, *J. Irrig. Drain. Eng.* 131(4), 316–323. DOI: 10.1061/~ASCE!0733-9437~2005!131:4~316!, 2005.
- UNEP, World atlas of desertification. 2nd ed. Edited by N. Middleton and D. Thomas. London: Arnold. 182 pp, 1997.
- 580 Vangelis, H., Tigkas, D., and Tsakiris, G.: The effect of PET method on Reconnaissance Drought Index (RDI) calculation. *J. Arid Environ.*, 88, 130–140. <http://dx.doi.org/10.1016/j.jaridenv.2012.07.020>, 2013.
- Villalobos, F.J., Mateos, L., and Fereres, E.; Irrigation Scheduling Using the Water Balance, In: Principles of Agronomy for Sustainable Agriculture, Villalobos, F.J. and Fereres, E, Springer International Publishing, Switzerland, 269–279, 2016.